THE UNIVERSITY OF ALABAMA® | University Libraries

The Formation and Evolution of Planetary Systems: First Results from a *Spitzer* Legacy Science Program

M. Silverstone – University of Arizona
et al.

Deposited 06/13/2019

Citation of published version:

Meyer, M.R., et al. (2004): The Formation and Evolution of Planetary Systems: First Results from a *Spitzer* Legacy Science Program. *The Astronomical Journal,* 154(1).
DOI: https://doi.org/10.1086/423177

© 2004. The American Astronomical Society. All rights reserved. Printed in U.S.A

The Astrophysical Journal Supplement Series, 154:422–427, 2004 September
© 2004. The American Astronomical Society. All rights reserved. Printed in U.S.A.

THE FORMATION AND EVOLUTION OF PLANETARY SYSTEMS: FIRST RESULTS FROM A *SPITZER* LEGACY SCIENCE PROGRAM

M. R. Meyer,[1] L. A. Hillenbrand,[2] D. E. Backman,[3] S. V. W. Beckwith,[4,5] J. Bouwman,[6] T. Y. Brooke,[2] J. M. Carpenter,[2] M. Cohen,[7] U. Gorti,[3] T. Henning,[6] D. C. Hines,[8] D. Hollenbach,[3] J. S. Kim,[1] J. Lunine,[9] R. Malhotra,[9] E. E. Mamajek,[1] S. Metchev,[2] A. Moro-Martin,[1] P. Morris,[10] J. Najita,[11] D. L. Padgett,[10] J. Rodmann,[6] M. D. Silverstone,[1] D. R. Soderblom,[4] J. R. Stauffer,[10] E. B. Stobie,[1] S. E. Strom,[11] D. M. Watson,[12] S. J. Weidenschilling,[13] S. Wolf,[6] E. Young,[1] C. W. Engelbracht,[1] K. D. Gordon,[1] K. Misselt,[1] J. Morrison,[1] J. Muzerolle,[1] and K. Su[1]

Received 2004 March 26; accepted 2004 May 20

ABSTRACT

We present 3–160 μm photometry obtained with the Infrared Array Camera (IRAC) and Multiband Imaging Photometer for *Spitzer* (MIPS) instruments for the first five targets from the *Spitzer Space Telescope* Legacy Science Program "Formation and Evolution of Planetary Systems" and 4–35 μm spectrophotometry obtained with the Infrared Spectrograph (IRS) for two sources. We discuss in detail our observations of the debris disks surrounding HD 105 (G0 V, 30 ± 10 Myr) and HD 150706 (G3 V, $\sim 700 \pm 300$ Myr). For HD 105, possible interpretations include large bodies clearing the dust inside of 45 AU or a reservoir of gas capable of sculpting the dust distribution. The disk surrounding HD 150706 also exhibits evidence of a large inner hole in its dust distribution. Of the four survey targets without previously detected IR excess, spanning ages 30 Myr to 3 Gyr, the new detection of excess in just one system of intermediate age suggests a variety of initial conditions or divergent evolutionary paths for debris disk systems orbiting solar-type stars.

Subject headings: circumstellar matter — infrared: stars — planetary systems: protoplanetary disks

1. INTRODUCTION

A combination of optical, infrared, and millimeter observations has provided incontrovertible evidence over the past two decades that most stars are surrounded at birth by circumstellar accretion disks (e.g., Beckwith & Sargent 1996). That at least some of these disks build planets has become clear from radial velocity and photometric studies revealing $M \sin i = 0.2\text{–}15 M_J$ planets orbiting nearby stars (e.g., Marcy et al. 2000). More indirect but still compelling evidence of planet formation comes from optical and infrared imaging of a few debris disks (e.g., Kalas et al. 2004 and Weinberger et al. 1999). These solar system–sized dust disks are comprised of micron-sized grains produced as by-products of collisions between asteroid-like bodies with orbits expected to be dynamically stirred by massive planets (e.g., Lagrange et al. 2000).

Following the *IRAS* discovery of excess infrared emission associated with Vega (Auman et al. 1984), *IRAS* and *ISO* identified several dozen debris disks around fairly luminous main-sequence stars. Neither observatory, however, had the sensitivity to detect *solar-type stars* down to photospheric levels at distances greater than a few pc, up to now preventing a complete census of solar-system–like debris disks over a wide ranges of stellar ages. The extant samples have made it difficult to infer the typical path of debris disk evolution (Habing et al. 1999; Meyer & Beckwith 2000; Spangler et al. 2001). The unprecedented sensitivity of the *Spitzer Space Telescope* (Werner et al. 2004) will enable the Legacy Science Program "The Formation and Evolution of Planetary Systems: Placing Our Solar System in Context" (FEPS) to search for debris systems around 330 stars with spectral types from F8 V to K3 V and ages ranging from 3 Myr to 3 Gyr. Observations and results described here are from early validation data taken with all three *Spitzer* instruments. Targets were selected from among those visible during the validation campaign of 2003 December to be representative of the overall FEPS sample, the primary control variable of which is stellar age. Observed were HD 105, HD 47875, HD 150706, HD 157664, and HD 161897 ranging in age from 30 Myr to 3 Gyr. We report here photometry for all of these stars and low-resolution spectrophotometry for two with observed IR excess, HD 105 and HD 150706.

Stellar properties for our validation sample are summarized here and reported in Table 1. HD 105 (G0 V, Houk 1978; 40 ± 1 pc, *Hipparcos*) is a kinematic member of the Tuc-Hor moving group (Mamajek et al. 2004). It is a coronally and chromospherically active dwarf star with youth established through its Li I λ6707 equivalent width (e.g., Wichmann et al. 2003), its position in the HR diagram, and activity indicators such as X-ray emission (Cutispoto et al. 2002) and Ca II HK emission (Wright et al. 2004). We adopt an age of 30 ± 10 Myr for HD 105. HD 150706 (G3 V, Buscombe 1998; 27 ± 0.4 pc, *Hipparcos*) is an active main-sequence dwarf with chromospheric Ca II HK emission (Wright et al. 2004) suggesting an age of 635–1380 Myr adopting the calibration of Donahue 1993 and coronal X-ray emission (Voges et al. 1999). The Li I λ6707 equivalent width (e.g., Soderblom et al. 1993)

[1] Steward Observatory, University of Arizona, 933 North Cherry Avenue, Tucson, AZ 85721.
[2] Astronomy, California Institute of Technology, Pasadena, CA 91125.
[3] NASA Ames Research Center, Moffet Field, CA 94035.
[4] Space Telescope Science Institute, Baltimore, MD 21218.
[5] Johns Hopkins University, Balitmore, MD 21218.
[6] Max-Planck-Institut für Astronomie, D-69117 Heidelberg, Germany.
[7] Radio Astronomy, University of California, Berkeley, CA 94720.
[8] Space Science Institute, Boulder, CO 80301.
[9] Lunar Planetary Laboratory, University of Arizona, Tucson, AZ 85721.
[10] *Spitzer* Science Center, California Institute of Technology, Pasadena, CA 91125.
[11] National Optical Astronomy Observatory, Tucson, AZ 85719.
[12] Department of Physics and Astronomy, University of Rochester, Rochester, NY 14627.
[13] Planetary Science Institute, Tucson, AZ 85719.

TABLE 1
ADOPTED STELLAR AND DERIVED CIRCUMSTELLAR PROPERTIES

Name	Spectral Type	$T_{\rm eff}$[a] (K)	$\log (L_*/L_\odot)$[a]	$\log g$[a]	A_V[a] (mag)	τ/Myr[b]	d[b] (pc)	$\log L_{\rm IR}/L_*$	$M_{\rm dust}$[c] ($M_\odot$)	$R_{\rm in}$[c] (AU)	$R_{\rm out}$[c] (AU)
HD 105	G0 V	6063	0.11	4.47	0.00	30 ± 10	40 ± 1	-3.41	$\sim 1.0 \times 10^{-7}$	45.0	...
HD 47875	G3 V	5886	0.10	4.61	0.36	30–200	70	<-3.85	$<1.8 \times 10^{-7}$	...	...
HD 150706	G3 V	5958	-0.03	4.62	0.00	700 ± 300	27 ± 0.4	-4.27	$\sim 6.9 \times 10^{-8}$	20	<100
HD 157664	G0	6494	0.63	4.50	0.18	1000–3000	84 ± 5	<-4.22	$<6.1 \times 10^{-8}$	...	...
HD 161897	K0	5579	-0.18	4.50	0.00	1000–3000	29 ± 1	<-4.31	$<6.3 \times 10^{-8}$	...	...

[a] Based on the photospheric model fitting procedure described in the text.
[b] Derived from data taken from the literature.
[c] Based on the circumstellar disk models described in the text.

indicates an age consistent with possible kinematic membership in the UMa group (e.g., King et al. 2003) of ~300–500 Myr. We adopt the weighted average of these two age estimates, 700 ± 300 Myr for HD 150706. HD 47875 is a young active X-ray emitting star (Favata et al. 1995) with kinematics consistent with membership in the local association. We assign an age of 30–200 Myr to this source. HD 157664 is a galactic disk field star. Because there are no indications of youth and because volume-limited samples of Sunlike stars are most likely 1–3 Gyr old (e.g., Rocha-Pinto et al. 2000), we tentatively assign this age to HD 157664. HD 161897 is similarly inactive, and we assign a preliminary age based on its Ca II HK emission (Wright et al. 2004) of 1–3 Gyr.

2. *SPITZER SPACE TELESCOPE* DATA

Next we describe the data acquisition and reduction strategies for each instrument. The derived flux densities for all five sources are presented in Table 2.

Infrared Array Camera (IRAC) (Fazio et al. 2004) observations in each of the four channels used the 32×32 pixel subarray mode with an effective integration time of 0.01 s per image (frame time of 0.02 s). The 64 images at each position in the four-point random dither pattern provided a total integration time of 2.56 s per channel. We began with the Basic Calibrated Data (BCD) products of the *Spitzer* Science Center (SSC) S9.1 data pipeline as described in the *Spitzer* Observer's Manual version 4.0 (hereafter SOM[14]). Aperture photometry was performed using IDP3 (Schneider & Stobie 2002) version 2.9. We used a 2 pixel radius aperture centered on the target and estimated background beyond an 8 pixel radius as the median of ~820 pixels. Background flux was normalized to the area of the target aperture and subtracted from the summed target flux. The final source flux is the median of the 256 measures, corrected from a 2 pixel radius to the 10 pixel radius used for the IRAC instrumental absolute flux calibration. Measurement uncertainty was estimated as the standard error in the mean and added in quadrature to an absolute flux calibration uncertainty of 10%.

Low-resolution ($\lambda/\Delta\lambda \simeq 70$–$120$) spectra were obtained with the Infrared Spectrograph (IRS) (Houck et al. 2004) over the entire wavelength range available (5.2–38 μm) for all validation targets. We present here reduced spectral observations in Figure 1 for HD 105 and HD 150706 only. We used an IRS high-accuracy blue peak-up to acquire the source in the spectrograph slit. Integration times per exposure were 6 s over the Short-Low wavelength range (5.2–14.5 μm), and either 6 s (HD 150706) or 14 s (HD 105) over the Long-Low wavelength range (14.0–38.0 μm). One cycle, resulting in spectra at two nod positions, was obtained in staring mode for averaging and estimating the noise. The BCDs resulting from the SSC pipeline S9.1 were reduced within the SMART software package (Higdon et al. 2004, in preparation). We used the *droopres* data products before stray-light and flat-field corrections were applied. Spectra were extracted assuming point source profiles with a fiducial width of 5–6 pixels in the center of the orders but allowing for variable width to account for increasing PSF size as a function of wavelength. Residual emission (mostly due to solar system zodiacal dust) was subtracted using adjacent pixels. The background-subtracted spectrum was divided by the spectrum of a photometric standard star (α Lac) and multiplied by an appropriately binned template spectrum for this standard provided by the IRS instrument team. Random errors calculated from the difference between the two independent spectra were added in quadrature with an estimated 15% uncertainty in absolute flux calibration to produce the spectra shown in Figure 1.

Multiband Imaging Photometer for *Spitzer* (MIPS; Rieke et al. 2004) observations were obtained in all three bands using the small field photometry mode with two cycles of 3 s Data Collection Events (DCEs) at 24 μm and two cycles of 10 s

[14] See http://ssc.spitzer.caltech.edu/documents/som/.

TABLE 2
Spitzer PHOTOMETRY IN mJy

Source	3.6 μm	σ	4.5 μm	σ	5.8 μm	σ	8.0 μm	σ	24 μm	σ	70 μm	σ	160 μm	σ
HD 105	960	96	610	61	427	43	222	22	28.0	3.0	142	29	227	91
HD 47875	327	33	210	21	153	16	77	8	9.4	1.1	<18	NA	<42	NA
HD 150706	1587	159	1014	102	697	70	377	38	44.2	4.5	36	9	<52	NA
HD 157664	582	58	368	37	252	25	133	13	15.0	1.7	<18	NA	<36	NA
HD 161897	1142	114	715	72	495	50	266	27	29.5	3.1	<19	NA	<35	NA

NOTE.—Fluxes quoted are based on the calibrations used in the SOM vers. 4.0. Errors quoted are derived as discussed in the text including calibration uncertainties. Upper limits are 3 σ as discussed in the text.

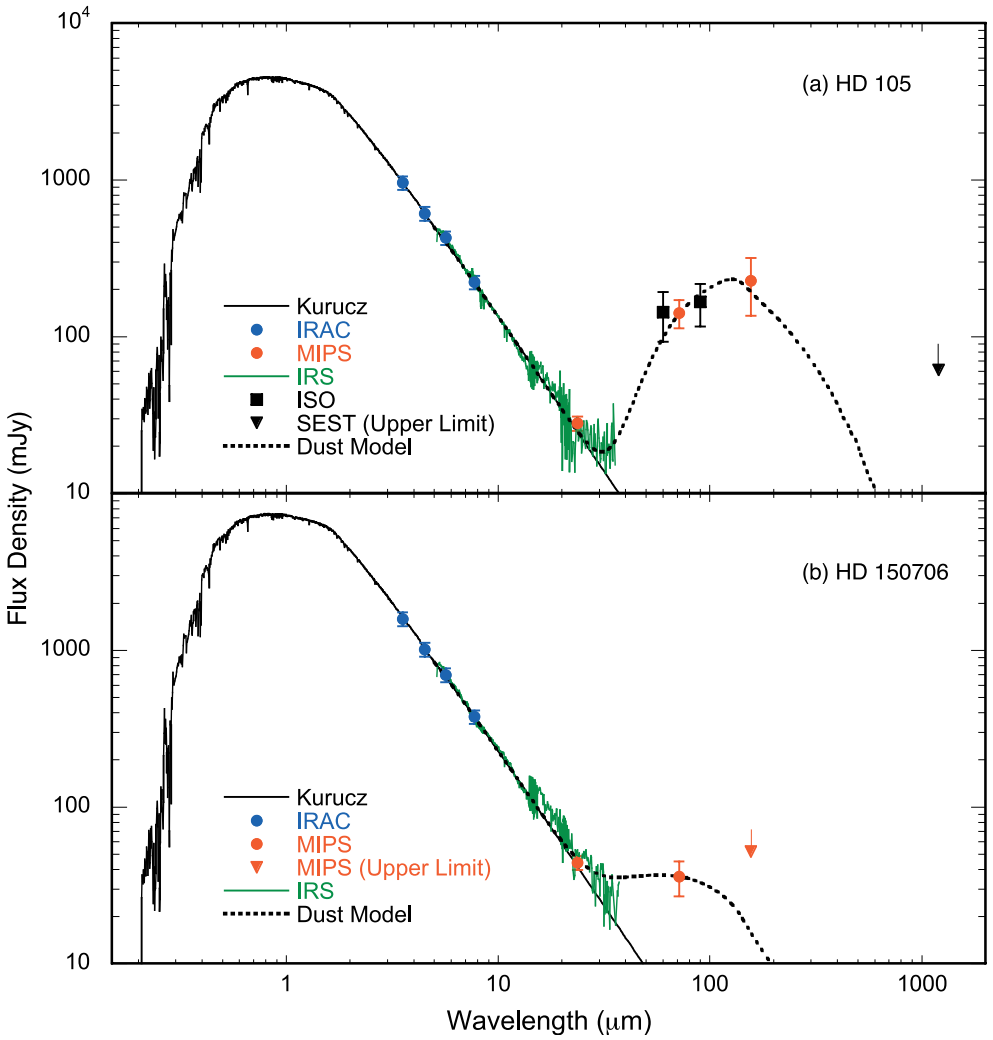

FIG. 1.—Spectral energy distributions for HD 105 and HD 150706 using data from Table 2 and stellar models from Table 1. Also shown are representative models for the dust debris disks surrounding HD 105 ($R_{in}/R_{out} = 45/300$ AU; $a_{min}/a_{max} = 5/100$ μm) and HD 150706 ($R_{in}/R_{out} = 20/100$ AU; $a_{min}/a_{max} = 1/100$ μm) discussed in the text.

DCEs at 160 μm, approaching the confusion limit (Dole et al. 2004). At 70 μm, we observed HD 105, HD 150706, and HD 161897 for two cycles, HD 157664 for four cycles, and HD 47875 for seven cycles all with 10 s DCEs. After initial processing by the SSC S9.1 pipeline to provide reconstructed pointing information, the MIPS data were further reduced using the MIPS Data Analysis Tool (DAT, ver. 2.71) developed by the MIPS Instrument Team (Gordon et al. 2004). This includes the "enhancer" portion of the DAT, which corrects for distortion in individual images and combines them onto a subsampled tangential plane mosaic. We present images of HD 105 and HD 150706 at 70 and 160 μm in Figure 2 (Plate 1). Aperture photometry was performed in IDP3 with target apertures of 14.″99, 29.″70, and 47.″8 at 24, 70, and 160 μm, respectively. We used background annuli of 29.″97–42.″46 for 24 μm, 39.″6–79.″2 for 70 μm, and 47.″9–79.″8 for 160 μm. The mean background per pixel was scaled to the appropriate aperture size and subtracted from the summed flux inside each aperture. Random uncertainties were determined from the ensemble of measurements for the 24 μm observations and from the noise in the background for the mosaicked images at 70 and 160 μm. These error estimates were added in quadrature with uncertainties in the absolute calibration of 10%, 20%, and 40% for 24, 70, and 160 μm, respectively, as measured for sources as faint as 60 mJy as 70 μm. Upper limits were derived for sources not detected based on photometry attempted at the source position estimated from the coordinates given in the image headers. Three times the estimated noise was used to determine an upper limit if the inferred SNR of the measured flux was less than 3 σ.

3. SPECTRAL ENERGY DISTRIBUTIONS OF TARGETS

We present SEDs for HD 105 and HD 150706 in Figure 1. We have adopted the recommended (SOM) central wavelengths and have not applied color corrections that are still uncertain and much smaller than the quoted absolute calibration uncertainties. The photospheric emission component was modeled by fitting Kurucz atmospheres including convective overshoot to available *BV* Johnson, *vby* Stromgren, $B_T V_T$ Tycho, H_p *Hipparcos*, *RI* Cousins, and *J*, *H*, K_s 2MASS photometry. Predicted magnitudes were computed as described in Cohen et al. (2003 and references therein) using the combined system response of filter, atmosphere (for ground-based observations), and detector. The best-fit Kurucz model was computed in a least squares sense with the effective temperature and normalization constant (i.e., radius) as free parameters, [Fe/H]

fixed to solar metallicity, and surface gravity fixed to the value appropriate for the adopted stellar age and mass. Visual extinction was fixed to $A_V = 0$ mag for stars with distances less than 40 pc, assumed to be within the dust-free Local Bubble, but a free parameter for HD 47875 and HD 157664. The adopted stellar parameters are listed in Table 1.

Emission in excess of that expected from the stellar photospheres is found in two of our five validation targets, HD 105 and HD 150706. The remaining three validation targets have no significant excess emission and were not detected at 70 μm despite sensitivities comparable to the HD 105 and HD 150706 observations. We place limits on the ratio $L_{\rm IR}/L_*$ for these three stars based on the observed upper limits (assuming a dust temperature of $\sim$40 K) in Table 1 and discuss the two excess sources in detail.

HD 105 was found to have an IR excess by Silverstone (2000) based on 60 and 90 μm *ISO* ISOPHOT measurements. We confirm that with *Spitzer* measurements of excess at 70 and 160 μm but find no obvious excess at $\lambda < 35$ μm based on the IRS spectra or IRAC/MIPS photometry. The total flux in the excess calculated via trapezoidal integration from 24 to 1200 μm is $\sim 1 \times 10^{-14}$ W m^{-2}, corresponding to $L_{\rm IR}/L_* \sim 3.9 \times 10^{-4}$. Assuming a temperature of $\sim$40 K, the estimated solid angle subtended by total effective particle cross section is $\sim 2 \times 10^{-13}$ sr $= 13$ AU^2 for $d = 40$ pc. Based on the 24 μm measurement, we estimate there can be no more than 3×10^{-3} as much radiating area at 100 K, and no more than 4×10^{-5} as much at 300 K, as there is at 40 K. HD 150706 has a newly discovered IR excess at 70 μm, but only an upper limit at 160 μm and no evidence for excess at $\lambda < 35$ μm. The total flux in the excess is $\sim 3 \times 10^{-15}$ W m^{-2}, corresponding to fractional IR luminosity $\sim 5.4 \times 10^{-5}$. Assuming a temperature of less than 84 K, the total effective particle cross section is more than 0.09 AU^2 for $d = 27$ pc.

4. DISK PROPERTIES AND INTERPRETATION

Following arguments employed for Vega and the other main-sequence debris disk archetypes discovered by *IRAS* (Backman & Paresce 1993), we assume the IR excess emission around HD 105 and HD 150706 is from grains orbiting, and in thermal equilibrium with radiation from, the central stars. Model inner and outer radii for disks containing the cold material around HD 105 and HD 150706 can be calculated with assumptions regarding grain composition, size distributions, and spatial distributions. The lack of distinct mineralogical features in the observed IRS spectra (which would constrain the dust properties) means there can be no unique model but rather a range of models that satisfy the observations. For HD 150706 the single data point for the IR excess translates into a limit that the material must lie farther from the star than $\sim$11 AU if it is in the form of "blackbody" grains larger than the longest wavelength of significant emission. Smaller grains would satisfy the same temperature constraint at larger distances from the star. The material around HD 105 is consistent with being distributed in a narrow ring with inner edge $R_{\rm in}$ at 42 ± 6 AU and an outer edge at $R_{\rm out} - R_{\rm in} < 4$ AU if "blackbody" grains are assumed. The ranges result from photometric uncertainty and are independent of the assumed grain surface density radial power-law exponent within the range $\Sigma(r) \sim r^{[-2.0,\ 0]}$. If material in the inner "hole" is assumed to have constant surface density with radius (as would be produced through the Poynting-Robertson [P-R] effect), the surface density in the zone at $r < R_{\rm in}$ is less than 3×10^{-2} of the model surface density at $r > R_{\rm in}$. Another family of models containing intermediate-sized (graybody) grains with emissivity falling as $1/\lambda$ beyond $\lambda = 40$ μm possesses inner edges $R_{\rm in}$ ranging from about 50 to 70 AU and outer edges $R_{\rm out}$ ranging from 250 to 1500 AU depending on the assumed radial power-law exponent of the surface density distribution.

Given the above results for HD 105 and HD 150706 from simple models with strong (but reasonable) assumptions about the grain properties of the observed disks, we now explore ranges of disk models that are consistent with the data following Wolf & Hillenbrand (2003). For grain compositions we assumed "astronomical" silicate plus graphite in the ISM ratio and surface density distribution $\Sigma(r) \propto r^0$. The mass of the disk was adjusted to match the peak flux in the infrared excess. Parameters such as grain size distribution $n(a) \sim a^{-p}$ power-law exponent, minimum/maximum grain size, and the inner/outer edge of the disk, were varied to find the range of values consistent with the observed spectral energy distribution of HD 105. The models were relatively insensitive to the radial density distribution exponent. The wavelength at which the dust reemission spectrum begins to depart significantly from the stellar photosphere was used to find the smallest grain size and smallest inner disk radius consistent with the data. These two parameters are degenerate resulting in single grain sizes in the range 0.3, 5, and 8 μm requiring inner gap sizes of 1000, 120, and 42 AU, respectively. Adopting a minimum grain size of 5 μm and allowing for a grain size distribution up to 100 or 1000 μm produced lower χ^2 fits and decreased the required inner radius from 120 to 45 AU (32 AU for $a_{\rm min} \sim 8$ μm or larger). The upper grain size, if one exists, and the outer radius are not well constrained in the absence of submillimeter measurements. The mass in grains of less than 1 mm for the above models is between 9×10^{-8} and 4×10^{-7} $M_\odot$. For HD 150706, we used the measured 70 μm flux and 160 μm upper limit and the methodology outlined above to model the disk. Compared to HD 105, we find a smaller minimum grain size (0.3 or 1 μm) and a narrower disk (inner radius $\sim$45 or $\sim$20 AU, respectively, with outer radius $<$100 AU). For the remaining three objects, we used the best-fit model for HD 150706 and scaled the results to the observed upper limits on $L_{\rm IR}/L_*$ to derive the dust mass upper limits given in Table 1.

In the cases of our two disk detections, assuming a grain density[15] of 2.5 g cm^{-3} we can calculate the P-R drag timescale. For HD 105 removal of 5 μm grains occurs $<$15 Myr at 45 AU compared to a stellar age of 30 Myr, suggesting that any such small grains are regenerated, perhaps through collisions of planetesimals. However, given the optical depth of the dust (15–300 AU^2, the radiating cross-sectional area), the timescale for dust grains to collide is less than 10^6 yr, suggesting that collisions as well as P-R drag are important in determining the actual size distribution of the dust as well as its radial surface density profile. For HD 150706 the P-R drag timescale for 1 μm grains at 20 AU is less than 1 Myr compared to an age of 700 ± 300 Myr, suggesting regeneration of dust through collisions of planetesimals as in the case of HD 105. In both cases the lack of circumstellar material in the inner disk (expected from a model of P-R drag) suggests that (1) something is preventing dust at 20–45 AU from reaching the sublimation radius in the inner disk and (2) a lack of significant numbers of colliding planetesimals inside of 20–45 AU. This suggests that the inner region is relatively clear of small

[15] This density is appropriate for solid silicate dust grains, which we assume are the result of comminuted Kuiper Belt object or cometary analogs whose bulk densities are lower.

bodies, consistent with some estimates for the timescale of terrestrial planet formation (e.g., Kenyon & Bromley 2004). The presence of one or more large planets interior to ~20–45 AU may explain the inner edge of the outer dust disk (e.g., Moro-Martín & Malhotra 2003). The preceding discussion presumed that the gas-to-dust mass ratio is less than 0.1, for which the dust dynamics are driven by interactions with the radiation field of the central star. Our high-resolution IRS observations of the ~30 Myr star HD 105, still under analysis, should be sensitive to small amounts of gas between 50 and 200 K. The presence of a remnant inner gas disk can influence dust migration and produce a ring morphology such as we infer for the dust (Takeuchi & Artymowicz 2001).

HD 150706, with an age of 700 ± 300 Myr, is less likely to retain a gas-rich disk than HD 105 (e.g., Zuckerman et al. 1995). However, it does exhibit evidence for a previously undetected dust disk, while HD 47875, HD 157664, and HD 161897, ranging in age from 30 Myr to 3 Gyr, do not at levels comparable to the HD 150706 detection (Table 1). The disk surrounding HD 150706 has a hole devoid of dust with inner radius of at least 20 AU, comparable to the disk surrounding HD 105. Perhaps the inner region of this disk is being kept clear by the presence of larger bodies as discussed above. While we cannot draw robust conclusions from these small samples, it is clear that other factors (range in primordial disk properties and/or variations in evolutionary histories?) are required to explain the growing body of debris disk observations besides a simple monotonic decrease in dust mass with age.

We would like to thank our colleagues at the *Spitzer* Science Center and members of the instrument teams for their help in analyzing the *Spitzer* data. FEPS is pleased to acknowledge support through NASA contracts 1224768, 1224634, and 1224566 administered through JPL.

REFERENCES

Aumann, H. H., et al. 1984, ApJ, 278, L23
Backman, D. E., & Paresce, F. 1993, in Protostars and Planets III, ed. E. Levy & J. I. Lunine (Tucson: Univ. Arizona Press), 1253
Beckwith, S. V. W., & Sargent, A. I. 1996, Nature, 383, 139
Buscombe, W. 1998, 13th General Catalogue of MK Spectral Classification, VizieR Online Data Catalog, 3206, 0
Cohen, M., Megeath, S. T., Hammersley, P. L., Martín-Luis, F., & Stauffer, J. 2003, AJ, 125, 2645
Cutispoto, G., Pastori, L., Pasquini, L., de Medeiros, J. R., Tagliaferri, G., & Andersen, J. 2002, A&A, 384, 491
Dole, H., et al. 2004, ApJ, submitted
Donahue, R. A., 1993, Ph. D. thesis, New Mexico State Univ.
Favata, F., Barbera, M., Micela, G., & Sciortino, S. 1995, A&A, 295, 147
Fazio, G., et al. 2004, ApJS, 154, 10
Gordon, K. D., et al. 2004, PASP, submitted
Habing, H. J., et al. 1999, Nature, 401, 456
Houck, J., et al. 2004, ApJS, 154, 18
Houk, N. 1978, Michigan Catalogue of Two-dimensional Spectral Types for the HD Stars (Ann Arbor : Univ. Michigan; distributed by University Microfilms International)
Kalas, P., Liu, M. C., & Matthews, B. C. 2004, Science, 303, 1990
Kenyon, S. J., & Bromley, B. C. 2004, ApJ, 602, L133
King, J. R., Villarreal, A. R., Soderblom, D. R., Gulliver, A. F., & Adelman, S. J. 2003, AJ, 125, 1980
Lagrange, A.-M., Backman, D. E., & Artymowicz, P. 2000, in Protostars and Planets IV, ed. V. Mannings, A. P. Boss, & S. S. Russell (Tucson: Univ. Arizona Press), 639
Mamajek, E. E., et al. 2004, ApJ, 612, 496
Marcy, G. W., Cochran, W. D., & Mayor, M. 2000, in Protostars and Planets IV, ed. V. Mannings, A. P. Boss, & S. S. Russell, (Tucson: Univ. Arizona Press), 1285
Meyer, M. R., & Beckwith, S. V. W. 2000, in *ISO* Survey of a Dusty Universe, ed. D. Lemke, M. Stickel, & K. Wilke (Berlin: Springer), 341
Moro-Martín, A., & Malhotra, R. 2003, AJ, 125, 2255
Rieke, G. H., et al. 2004, ApJS, 154, 25
Rocha-Pinto, H. J., Maciel, W. J., Scalo, J., & Flynn, C. 2000, A&A, 358, 850
Schneider, G., & Stobie, E. 2002, in ASP Conf. Ser. 281, ADASS XI, ed. D. A. Bohlender, D. Durand, & T. H. Handley (San Francisco: ASP), 382
Silverstone, M. D. 2000, Ph.D. thesis, UCLA
Soderblom, D. R., Pilachowski, C. A., Fedele, S. B., & Jones, B. F. 1993, AJ, 105, 2299
Spangler, C., Sargent, A. I., Silverstone, M. D., Becklin, E. E., & Zuckerman, B. 2001, ApJ, 555, 932
Takeuchi, T., & Artymowicz, P. 2001, ApJ, 557, 990
Voges, W., et al. 1999, *ROSAT* All-Sky Bright Source Catalogue, VizieR Online Data Catalog, 9010, 0
Weinberger, A., et al. 1999, ApJ, 525, L53
Werner, M. W., et al. 2004, ApJS, 154, 1
Wichmann, R., Schmitt, J. H. M. M., & Hubrig, S. 2003, A&A, 399, 983
Wolf, S., & Hillenbrand, L. A. 2003, ApJ, 596, 603
Wright, J. T., Marcy, G. M., Butler, R. P., & Vogt, S. S. 2004, ApJS, 152, 261
Zuckerman, B., Forveille, T., & Kastner, J. H. 1995, Nature, 373, 494

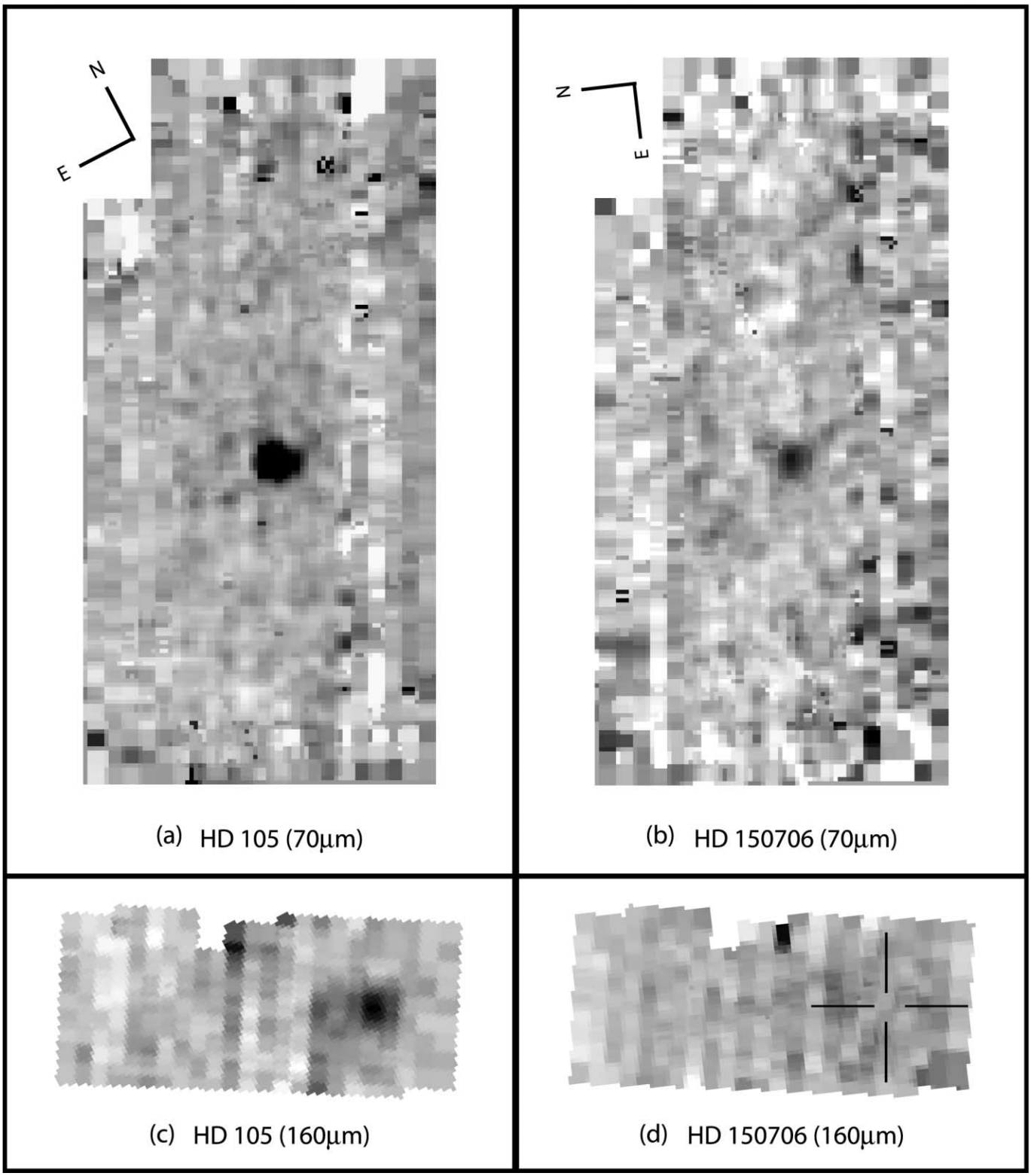

FIG. 2.—MIPS 70 and 160 μm images from which photometry was derived. These images have been four times oversampled.

PLATE 1